RESEARCH ARTICLE

Hypoxia-Inducible Factor-1α and the Glycolytic Phenotype in Tumors[1]

Ian F. Robey, Anthony D. Lien, Sarah J. Welsh, Brenda K. Baggett and Robert J. Gillies

Department of Biochemistry and Molecular Biophysics, University of Arizona Cancer Center, Tucson, AZ, USA

Abstract

Metastatic tumors generally exhibit aerobic glycolysis (the Warburg effect). The advent of [^{18}F]fluorodeoxyglucose positron emission tomography imaging, coupled with recent findings linking hypoxia-inducible factor (HIF-1α) overexpression to aggressive cancers, has rekindled an interest in this aspect of tumor metabolism. These studies explore the role of HIF-1α in human breast cancer lines and its relationship to glycolytic regulation. Here we demonstrate that, under normal oxygen conditions, nonmetastatic cells consume less glucose and express low HIF-1α, whereas metastatic cells constitutively express high glycolysis and HIF-1α, suggesting that dysregulation of HIF-1α may induce the Warburg effect. This hypothesis was tested by renormalizing HIF-1α levels in renal carcinoma cells, leading to inhibition of aerobic glycolysis.
Neoplasia (2005) **7**, 324–330

Keywords: Warburg effect, hypoxia-inducible factor, glucose consumption, lactate, glycolysis.

Introduction

Warburg [1] first established a correlation between aggressive tumor phenotypes and elevated glycolysis when he observed that many tumors produce excessive levels of lactic acid even in the presence of oxygen. Interest in the regulation of tumor glycolysis was rekindled, in part, due to thousands of [^{18}F]fluorodeoxyglucose positron emission tomography ([^{18}F]FdG-PET) patient scans demonstrating that a vast majority (>90%) of metastatic tumors are highly glycolytic [2,3]. The glycolytic phenotype expressed in metastatic cancers may be selected in periods of cyclic hypoxia during early tumor growth [4]. In this model, cells expressing constitutively high glycolysis survive bouts of ischemia characteristic of tumor perfusion [5]. Many tumors contain intermittently hypoxic microenvironments due to poor perfusion from an irregular and inefficient vasculature [6]. Furthermore, tumor hypoxia has been associated with cancer progression and resistance to radiation and chemotherapies, despite the fact that high microvessel density is also linked to poor prognosis [4,7,8]. This apparent dichotomy is likely explained by the observation that excessive angiogenesis leads to vascular imbalance and poor perfusion [9]. Acute hypoxia causes increased glycolysis at the substrate level (the Pasteur effect), likely mediated through intracellular redox balance. In contrast, chronic hypoxia can lead to high rates of glycolysis through stabilization of a hypoxia-inducible transcription factor, hypoxia-inducible factor (HIF-1α).

The recent discovery and study of HIF-1α have implicated a possible molecular mechanism for the Warburg effect in malignant tumors. First discovered by Semenza and Wang [10], HIF-1α plays an important role in cellular responses to hypoxia and other stresses. HIF-1α combines with HIF-1β to form a heterodimeric transcription factor that regulates the expression of glycolytic and angiogenic proteins. HIF-1α is constitutively expressed and destabilized in the presence of O_2 by proline hydroxylation and is targeted for proteosomal degradation by the von Hippel-Lindau (vH-L) ubiquitin ligase [11–15]. When accumulated (e.g., under hypoxia), the HIF-1 complex binds hypoxia response elements (HREs; canonically CCATG) in the promoter region of target genes. These include enzymes involved in glycolysis and pH regulation, such as phosphoglycerate kinase (PGK) [16], glucose transporters GLUT-1 and GLUT-3 [17,18], and carbonic anhydrase CA9 [19], as well as growth factors involved in angiogenesis and erythropoiesis, such as vascular endothelial growth factor (VEGF) [18,20] and erythropoietin (EPO) [10,21]. This is significant to the pathophysiology of tumors, as immunohistochemistry has shown that most metastatic cancers exhibit elevated levels of HIF-1α [22], which may be attributed to hypoxia or upregulated expression for survival purposes, even in a well-oxygenated environment [4].

This communication investigates the relationship between HIF-1α stabilization in oxygenated conditions and the Warburg effect. We explored this by comparing glucose transport, lactate production, HIF-1α protein, and HRE-induced transcript levels in metastatic (MDA-mb-435) and nonmetastatic (MCF-7) breast cancer lines. Under a 20% oxygen atmosphere (normoxia), MDA-mb-435 cells have elevated glycolysis, HIF-1α, and HRE transcripts, whereas these parameters

are measurably lower in MCF-7 cells. Hypoxia ($\leq$2% oxygen) induced no change in the glycolytic phenotype in MDA-mb-435 cells, whereas HIF-1α, HRE transcripts, and glycolysis were profoundly induced in MCF-7 cells.

Controversial findings have identified MDA-mb-435 cells with melanoma cells due to the expression of specific melanocyte genes [23] and lack of expression of breast cell line genes in MDA-mb-435 sublines [24]. To account for this possible discrepancy, we also included the MDA-mb-231 metastatic breast cell line for comparison to MCF-7 cells. We maintain the view, however, that MDA-mb-435 cells are breast epithelium cells that express melanocyte-specific genes from possible lineage infidelity during tumor progression [25].

Our findings were verified in examinations of a renal cell carcinoma (RCC4) where transfection of the vH-L gene into a vH-L−null line directly modulated HIF-1α levels. Parental RCC4 cells functioned similarly to the MDA-mb-435 and MDA-mb-231 lines by expressing high levels of HIF-1α and exhibiting high glycolysis under normoxic conditions. There was a minimal effect when these cells were switched to hypoxia. Restoration of vH-L activity led to normalization of the HIF-1α response. Under normoxia, RCC4/vH-L cells demonstrated low rates of glycolysis, which subsequently increased in hypoxia. Hence, these data implicate that dysregulation of HIF-1α can be a causal factor in the Warburg effect.

Materials and Methods

Cell Culture

MCF-7, MDA-mb-435, and MDA-mb-231 cells were obtained from the American Type Culture Collection (ATCC; Rockville, MD). The vH-L−null RCC4 (vH-L−transfected and vector-alone "mock"-transfected) cell lines were kindly donated by Garth Powis (Arizona Cancer Center, Tuczon, AZ). Cells were cultured in DMEM (Invitrogen, Carlsbad, CA) supplemented with 10% fetal calf serum (Omega Scientific, Inc., Tarzana, CA). Both RCC4 cell lines were selected and cultured in 400 μg/ml Geneticin (G418) (Gibco, Grand Island, NY). Exposure to hypoxia was carried out for 16 to 20 hours in $\leq$2% O_2, 93% N_2, and 5% CO_2 at 37°C.

Western Blot Analysis

Cells grown to approximately 80% confluence in 10-cm culture dishes were harvested for cytoplasmic protein. Cytoplasmic extracts were prepared according to the manufacturer's instructions included in NE-PER Nuclear and Cytoplasmic Extraction Reagents (Pierce, Rockford, IL). Protein concentration was assayed by Bradford assay (Pierce). Western blot analysis was performed as described previously [40]. Blots were probed overnight at 4°C, or for 2 hours at ambient temperature, with a 1:250 dilution of mouse antihuman HIF-1α (Transduction Laboratories, Lexington, KY) and a 1:1000 dilution of goat antihuman laminin (Santa Cruz Biotechnology, Santa Cruz, CA). Primary antibodies were followed by a 1:5000 dilution of horse-radish peroxidase−conjugated goat antimouse or donkey antigoat IgG secondary antibody (Santa Cruz Biotechnology) and developed using chemiluminescence kit (Amersham Pharmacia, Uppsala, Sweden).

Quantitative Real-Time PCR

Cells were incubated for approximately 20 hours in $\leq$2% O_2, 93% N_2, and 5% CO_2 (hypoxia) or 20% O_2, 75% N_2, and 5% CO_2 (normoxia). RNA was extracted using TRIZOL reagent (Invitrogen). Nucleic acid purity and concentration were measured on a spectrophotometer. Reverse transcription reaction was performed using the First Strand Synthesis kit (Invitrogen). Four micrograms of RNA was used in each RT reaction, and oligo dTs were used as primers. The cDNA was diluted with an equal part of filter-sterilized H_2O. Real-time PCR was performed with a light cycler (Cepheid, Foster City, CA) using SYBR Green reporter dye and Platinum Taq enzyme (Invitrogen). Two microliters of each cDNA sample was used per reaction. Primers (Table 1) were designed using the GCG/SeqLab http://bcf.arl.arizona.edu/gcg.html) and Primer3 (http://www-genome.wi.mit.edu) software. β-Actin, which was normalized between the cells lines with 18S RNA primers (forward: atcaactttcgatggtagtcg; reverse: ggcacacgcagctcattg), was used as the control gene for these experiments. Expression levels were determined as described previously using the following formula [41]: Relative gene expression $= 2^{([\beta\text{-actin } C_t] - [\text{target gene } C_t])}$. Statistical significance was determined by Student's t test.

Glucose Uptake Assay

Replicates of cells were seeded in assay plates and cultured in growth media to 80% confluency. For measurements of hypoxic glucose uptake rates, culture plates were transferred to a hypoxic incubator for 20 hours prior to assay. Cells were then washed in glucose-free RPMI 1640 media supplemented with 12 mM $NaHCO_3$. Glucose-free wash media for cells to be assayed in hypoxia were also treated with a 100-μM dilution of deferoxamine mesylate (DFO) iron-chelating reagent (Sigma, St. Louis, MO). Cells were then treated with 4 μCi of [^{3}H]2-deoxy-D-glucose (2dG) in RPMI 1640 media supplemented with 5.56 mM D-(+)-glucose and 12 mM $NaHCO_3$ and incubated in normoxia or hypoxia. Postincubation supernatant was sampled for liquid scintillation counting (LSC) using a 5000TD series liquid scintillation counter (Beckman Coulter, Inc., Brea, CA). Cells were washed three times in glucose-free media and lysed with 0.1 N NaOH for 1 minute. A lysate fraction was sampled for LSC. The remaining lysate was neutralized with 0.1 N

Table 1. Primer Sequences.

Gene	Forward Primer (5′−3′)	Reverse Primer (5′−3′)
PGK	aggaagaagggaagggaaaag	tcatcaaaaacccaccagc
GLUT-1	tcaatgctgatgatgaacctgct	ggtgacacttcacccacataca
GLUT-3	gacagcccatgcatcatttcc	gaacaaaaagccatccctcc
EPO	gtcccagacaccaaagttaa	aggccactgacggctttat
VEGF	gtccaacatcaccatgcag	gcaagtacgttcgtttaactc
CA9	ctttgaatgggcgagtgatt	tctcatctgcacaaggaacg

HCl and assayed for protein concentration using Bradford reagent (Pierce). Statistical significance was determined by Student's *t* test.

Lactate Assay

Replicates of cells were seeded in assay plates and cultured in growth media to 80% confluency. Cells were washed three times with glucose-free RPMI supplemented with 12 mM NaHCO$_3$ and treated with RPMI 1640 media supplemented with 5.56 mM D-(+)-glucose and 12 mM NaHCO$_3$ and incubated for 16 hours in either hypoxic or normoxic conditions. The supernatant was assayed for lactate concentration using a lactate reagent (Sigma). Statistical significance was determined by Student's *t* test.

Results

Expression of HIF-1–Regulated Genes

The Western blot analysis in Figure 1*A* illustrates that HIF-1α levels in MCF-7 cells were low under normoxic conditions and elevated after 20 hours in hypoxia. In contrast, MDA-mb-435 and MDA-mb-231 cells expressed elevated HIF-1α levels under normoxic conditions, which

increased further after incubation in hypoxia. The internal β-actin controls exhibited no variation between normoxic and hypoxic conditions within each cell line tested. β-Actin expression levels differed between individual cell lines. This was also observed in the RNA expression studies, indicating that β-actin production in these cell lines was unaltered by any experimental variables. To investigate whether the HIF-1α was transcriptionally active in these cells, mRNA was extracted from MDA-mb-435, MDA-mb-231, and MCF-7 cells, and quantitative real-time polymerase chain reaction (qRT-PCR) was carried out using primers designed for the HIF-1α−inducible genes (Table 1). Results are provided in Figure 2. Under normoxia, GLUT-1, GLUT-3, PGK, EPO, and VEGF expressions were all increased in metastatic lines compared to MCF-7. GLUT-1 expression levels were three-fold higher in MDA-mb-435 and MDA-mb-231 than in MCF-7. The greatest difference was observed in GLUT-3, where MDA-mb-435 and MDA-mb-231 expression levels were elevated 400-fold over MCF-7 GLUT-3 transcripts. PGK expression levels, although significant, were only marginally higher in MDA-mb-435 (by a factor of 2) and MDA-mb-231 (by a factor of 1.5) compared to MCF-7. EPO transcripts were four- to six-fold elevated in the metastatic cells compared to MCF-7. VEGF mRNA expression was
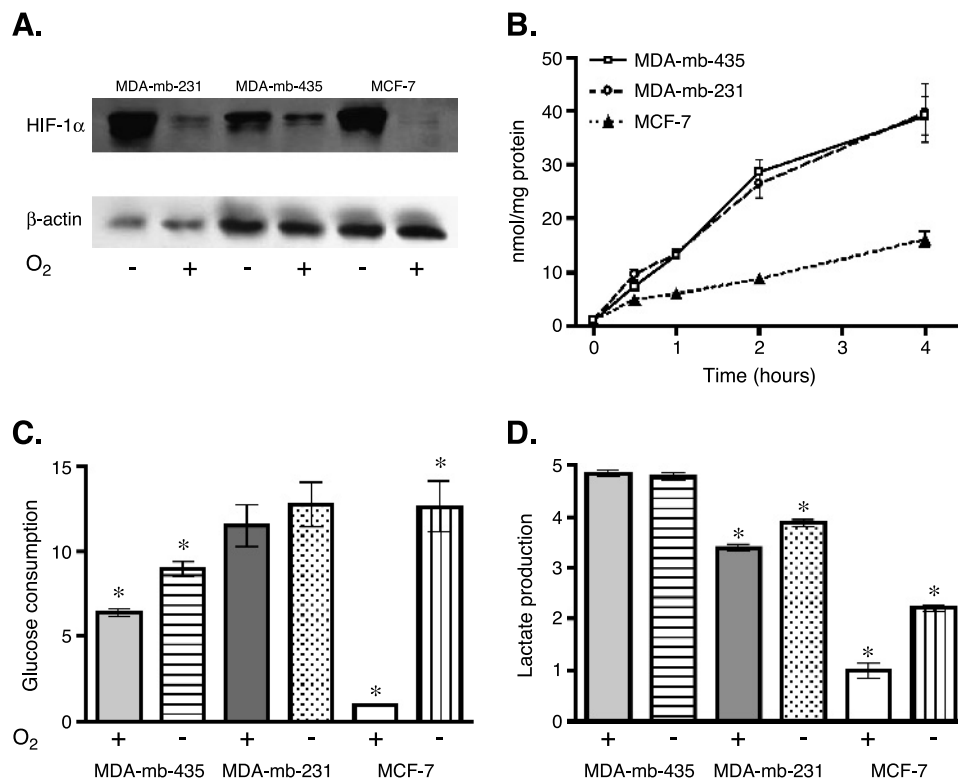

Figure 1. *HIF-1α expression and the glycolytic phenotype in MDA-mb-435, MDA-mb-231, and MCF-7 cells. (A) Western blots of HIF-1α with internal β-actin controls in MDA-mb-231, MDA-mb-435, and MCF-7 cells. Cells were exposed to hypoxia (≤2% oxygen; −) or normoxia (20% oxygen; +) for 16 hours. (B) Normoxic time course (240 minutes) of 2dG trapping in MDA-mb-435, MDA-mb-231, and MCF-7 cells. Glucose consumption rates were normalized from zero time point values and expressed as nanomoles per milligram of protein. (C) Normoxic and hypoxic 2dG trapping rates in MDA-mb-435, MDA-mb-231, and MCF-7 cells. Cells were grown under either normal (+) oxygen conditions (20%) or limiting (−) oxygen conditions (≤2%) in 2dG for 60 minutes. Glucose consumption values were normalized against normoxic uptake rate of MCF-7 cells. *Significant difference between expression of normoxia and hypoxia within each cell line (P < .05). (D) Normoxic and hypoxic lactate production. MDA-mb-435, MDA-mb-231, and MCF-7 cells were grown under either normal (+) oxygen conditions (20%) or limiting (−) oxygen conditions (≤2%) for approximately 16 hours. Lactate expression values were normalized against normoxic lactate production rate of MCF-7 cells. *Significant difference between expression of normoxia and hypoxia within each cell line (P < .05).*
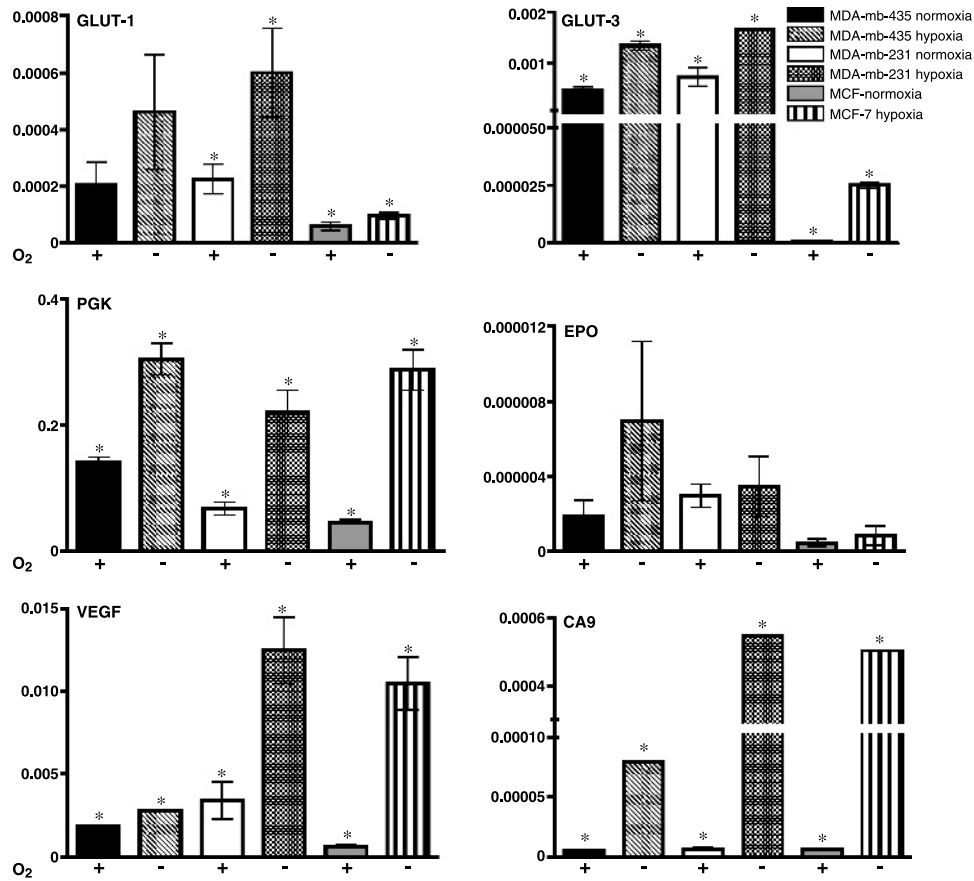
Figure 2. *HIF-1α–inducible gene expression in MDA-mb-435, MDA-mb-231, and MCF-7 cells. Cells were incubated under normoxia (+) or hypoxia (−), as described in the Materials and Methods section, for approximately 20 hours. Quantitative RT-PCR was carried out on extracted mRNA using primers for GLUT-1, GLUT-3, PGK, EPO, VEGF, and CA9. Ordinate values are based on standardization of target gene expression to that of β-actin. *Significant difference between expression of normoxia and hypoxia within each cell line (P < .05).*

increased by approximately three- to six-fold in the metastatic cells over MCF-7. No differences between the cell lines were observed for CA9 expression under normoxia. Normoxic gene expression between the two metastatic cells lines was similar in all genes tested, with the exception of PGK where MDA-mb-435 levels were twice those observed in MDA-mb-231.

Under hypoxia, all cells displayed significant increases in all transcripts except EPO. Hypoxic induction of GLUT-3 (>25-fold), PGK (>6-fold), and VEGF (>17-fold) was more dramatic in MCF-7 than induction levels observed in the metastatic cell lines. GLUT-3, PGK, VEGF, and CA9 transcripts were significantly induced by hypoxia in MDA-mb-435 cells. Transcript induction from hypoxia was similar between MDA-mb-231 and MDA-mb-435. GLUT-1 expression was also significantly induced in MDA-mb-231 cells by greater than 2.5-fold. The data from these experiments imply that GLUT-1 expression might be inducible under hypoxia in MDA-mb-435, but the results were not significant. All cell lines appeared to have relatively similar EPO and CA9 transcript levels under normoxia and hypoxia. These genes may have different thresholds for HIF-1α activation possibly due to the activity of other transcriptional activators or repressors. Comparing HIF-1α expression and transcript

levels between cell lines demonstrates that there is no strict correlation between transcript and HIF-1α levels, indicating differential regulation of mRNA levels for these genes in the assayed cell lines. Although not stoichiometric, these data show that expression of HIF-1–inducible genes is triggered by hypoxia (with the exception of EPO) to a greater extent in MCF-7, compared to MDA-mb-435 and MDA-mb-231 cells.

Glucose Uptake and Lactate Production in MDA-mb-435, MDA-mb-231, and MCF-7 Cells

Rates of glycolysis were investigated in MDA-mb-435, MDA-mb-231, and MCF-7 cells by monitoring the trapping of 2dG. These data demonstrate that 2dG trapping in MDA-mb-435 and MDA-mb-231 cells was significantly greater than that of MCF-7 cells under normoxic conditions. Glucose uptake rates were typically three-fold greater in MDA-mb-435 and MDA-mb-231 cells with respect to MCF-7 (Figure 1*B*). Figure 1*C* illustrates that 2dG trapping in MDA-mb-231 cells was not significantly different between normoxia and hypoxia. In MDA-mb-435 cells, there was a modest 1.4-fold increase in 2dG consumption under hypoxia, whereas the rate of 2dG trapping increased by over 12-fold in MCF-7 under hypoxic conditions. These results

were consistent with those reported earlier using a nonradioactive assay for glucose consumption [26].

Although trapping of 2dG is reflective of the changes taking place in [^{18}F]FdG-PET measurements, this endpoint is regulated only by glucose transporter (GLUT-1 or GLUT-3) and hexokinase activities and may not be indicative of overall glycolysis. Therefore, lactate production levels were also measured under normoxic and hypoxic conditions to determine if glycolysis was similarly affected. MDA-mb-435 cells produced lactate at similar levels under both normoxia and hypoxia, approximately five times the rate of MCF-7 cells under normoxia. MCF-7 cells, the lowest-expressing line under normoxia, significantly increased lactate production when exposed to hypoxia (approximately 2.2-fold). Metastatic cell line MDA-mb-231 demonstrated levels of lactate production three times the levels observed in MCF-7 cells under normoxia. These cells produced a small, but significant, increase (1.1-fold) in lactic acid when introduced to hypoxia in a manner similar to what was observed in MDA-mb435 glucose uptake experiments. Hence, both 2dG consumption and lactate production indicate that nonmetastatic MCF-7 cells have a "normal" metabolic response (i.e., low glycolysis under normoxia and a pronounced significant increase on hypoxia). In contrast, the metastatic MDA-

mb-435 and MDA-mb-231 cells exhibited the Warburg effect (i.e., high aerobic glycolysis). These behaviors are qualitatively similar to the differences in the HIF-1α levels observed in both cell lines. Aerobic HIF-1α levels were higher in MDA-mb-435 and MDA-mb-231 compared to MCF-7, concomitant with higher glycolytic rates. Interestingly, HIF-1α levels increased further in MDA-mb-435 and MDA-mb-231 cells under hypoxia, without a further increase in glycolysis. This suggests that glycolytic rates are maximally stimulated with only moderate increases in HIF-1α, and this is consistent with a high expression of the low K_m GLUT-3 transcript. It is also notable that HIF-1α levels in MCF-7 cells under hypoxia were higher than those in MDA-mb-435 and MDA-mb-231 cells under normoxia, yet glycolytic rates were lower. Thus, although these data suggest that HIF-1α might be involved in the regulation of the Warburg effect, the correlation is not exact and is likely to be cell type−dependent.

Glycolytic Phenotype in Renal Cell Lines Recapitulates Findings in Breast Cell Lines

To address this question, vH-L−null renal cell carcinoma (RCC4) cells were transfected to constitutively reexpress the vH-L enzyme. As shown in Figure 3A, RCC4 cells expressed elevated levels of HIF-1α under normoxia, attributable to
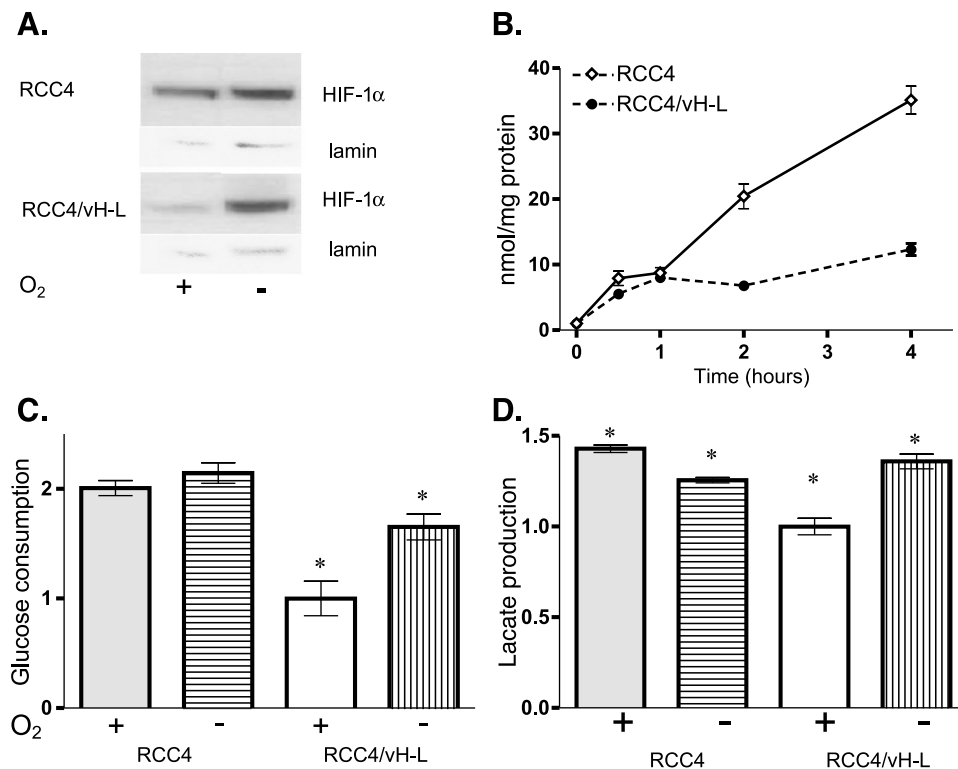

Figure 3. *HIF-1α expression and the glycolytic phenotype in RCC4 and RCC4/vH-L cells. (A) Western blots measuring HIF-1α with internal lamin controls in RCC4 and RCC4/vH-L cells under normoxia and hypoxia. Cells were exposed to hypoxia (≤2% oxygen; −) or normoxia (20% oxygen; +) for 16 hours. (B) Normoxic time course (240 minutes) of 2dG trapping in RCC4 and RCC4/vH-L cells. Glucose consumption rates were normalized from zero time point values and expressed as nanomoles per milligram of protein. (C) Normoxia and hypoxic 2dG trapping rates in RCC4 and RCC4/vH-L cells. RCC4 and RCC4/vH-L cells were grown under either normal (+) oxygen conditions (20%) or limiting (−) oxygen conditions (≤2%) in 2dG for 60 minutes. Glucose consumption values were normalized against normoxic uptake rate of RCC4/vH-L cells. *Significant difference between expression of normoxia and hypoxia within each cell line (P < .05). (D) Normoxic and hypoxic lactate expression. RCC4 and RCC4/vH-L cells were grown under either normal (+) oxygen conditions (20%) or limiting (−) oxygen conditions (≤2%) for approximately 16 hours. Lactate expression values were normalized against normoxic lactate production rate of RCC4/vH-L cells. *Significant difference between expression of normoxia and hypoxia within each cell line (P < .05).*

defective vH-L activity, and this was not affected by hypoxia. Reintroduction of vH-L activity with stable transfection restored "normal" destabilization of HIF-1α in the presence of oxygen, leading to low or absent levels under normoxia, which increased dramatically after incubation under hypoxia. These data are consistent with similar experiments performed previously [11].

Under normoxic conditions, the vH-L–null RCC4 cells exhibited 2dG trapping at an elevated rate similar to that seen in MDA-mb-435 and MDA-mb-231 cells, whereas the RCC4/vH-L cells demonstrated a 2dG uptake rate comparable to MCF-7 cells (Figure 3*B*). Similar to the metastatic cell lines, the vH-L–null RCC4 cells demonstrated no significant difference in 2dG trapping between normoxia and hypoxia, whereas the RCC4/vH-L transfectants were more akin to MCF-7 cells in that hypoxic glucose uptake increased almost two-fold over normoxia (Figure 3*C*). In both cell lines, lactate production rates correlated to the glucose consumption results (Figure 3*D*) in that RCC4 cells demonstrated higher normoxic lactate production than the vH-L transfectants and did not upregulate lactate production when grown under hypoxia, whereas a lactic acid increase was observed in the vH-L transfectants. These findings are consistent with a recent study wherein transfection of pancreatic cancer cell lines with a dominant-negative HIF-1α resulted in reduced aerobic glucose consumption [27]. In this same study, angiogenesis was unaffected, underscoring the functional relationship between HIF-1 activity and glycolysis.

Discussion

The current study indicates a causal role for HIF-1α in regulating glycolysis. Moreover, these data suggest that aerobic stabilization of HIF-1α could potentially drive glycolysis in tumors without dependence on a hypoxic environment. The incidence of HIF-1α stabilization under normoxic conditions in cancers is approximately 50%, as evidenced by our survey of cancer cell lines [28]. These findings and those in Figures 1*A* and 3*A* show that breast cancer lines MDA-mb-435 and MDA-mb-231, U87 glioblastoma, DU145 prostate cancer, and renal cell carcinomas RCC4 and CaKi express elevated HIF-1α under normoxic conditions. These cell lines are aggressively metastatic. In contrast, the more benign breast cancer MCF-7, HT-29 colon cancer, MiaPaCa pancreatic cancer, A549 lung cancer, and BX-PC3 prostate cancers do not accumulate measurable HIF-1α levels under normoxia. Although the cell lines exhibiting visible HIF-1α under normoxia are more metastatic, these data are too incomplete to imply an absolute correlation between HIF-1α dysregulation and aggressiveness. Nonetheless, within single cancers (i.e., for breast and prostate cancers), the more aggressive cell lines (MDA-mb-435, MDA-mb-231, and DU145, respectively) exhibit higher levels of normoxic HIF-1α, unlike the less vigorous cell lines (MCF-7 and BX-PC3, respectively). These data complement HIF-1α immuno staining showing that metastatic tumors were predominantly more positive compared to benign tumors [22]. In addition to glycolysis, constitutive ex-

pression of HIF-1α would have other sequelae such as dysregulated angiogenesis because both VEGF and its receptor, Flt-1, can be induced by HIF-1 activity [29]. Upregulation of these angiogenic factors may play a part in morphogenesis of chaotic vasculature, which is a hallmark of solid tumors [30]. The high normoxic expression of VEGF and other growth factors may be responsible for the correlation between microvessel density and tumor aggressiveness [31].

The mechanisms leading to accumulation of HIF-1α under normoxic conditions in MDA-mb-435 and MDA-mb-231 cells are unknown, and there are multiple possibilities. As with other breast cancers, MDA-mb-435 and MDA-mb-231 cells are unlikely to be vH-L–deficient [32], yet they may lack other components of the vH-L–mediated degradation pathway. HIF-1α accumulation could also occur by Ras, Src, and/or Akt oncogene expression, leading to inhibition of degradation or enhanced synthesis [33]. Increased constitutive rates of expression lead to higher steady-state HIF-1α levels even in the presence of active degradation. For example, tyrosine kinase (pp60^{c-Src}) transformation leads to increased frequency of HIF-1α protein synthesis, VEGF and PGK mRNA expression, and lactic acid production, whereas the HIF-1α degradation pathway remained functional [34]. Alternatively, HIF-1α stabilization could also occur through the augmented activity of the molecular chaperone, Hsp90 [35,36]. Finally, the glycolytic endproduct, pyruvate, promotes normoxic HIF-1α accumulation by preventing degradation in a manner similar to hypoxia [37].

The data in this study indicate that elevated HIF-1 activity is sufficient, but not necessary, for the Warburg effect. Other mechanisms resulting in glycolytic induction are possible. A recent report compared immunohistochemical staining patterns to [^{18}F]FdG uptake in a series of human tumors and showed a higher correlation with GLUT-1 expression compared to HIF-1α [38]. Hence, upregulated glucose transport may be more closely associated with the high glycolysis of the Warburg effect and elevated HIF-1α may be one of numerous mechanisms used to achieve this phenotype. The variable mechanisms used to enhance glycolysis, combined with the almost uniform observation of high FdG uptake in metastatic cancers, strongly suggest that elevated glycolysis is not merely an epiphenomenon of underlying molecular alterations, but is instead a key phenotype in cancer progression [4,39].

Conclusion

Dysregulated HIF-1α is responsible for the Warburg effect in some tumors.

References

[1] Warburg O (1956). On the origin of cancer cells. *Science* **123,** 309–314.
[2] Czernin J and Phelps ME (2002). Positron emission tomography scanning: current and future applications. *Annu Rev Med* **53,** 89–112.
[3] Gambhir SS, Czernin J, Schwimmer J, Silverman DH, Coleman RE, and Phelps MEA (2001). Tabulated summary of the FDG PET literature. *J Nucl Med* **42,** 1S–93S.
[4] Raghunand N, Gatenby RA, and Gillies RJ (2003). Microenvironmental

and cellular consequences of altered blood flow in tumors. *Br J Radiol* **76**, S11–S22.

[5] Kirkpatrick JP, Brizel DM, and Dewhirst MW (2003). A mathematical model of tumor oxygen and glucose mass transport and metabolism with complex reaction kinetics. *Radiat Res* **159**, 336–344.

[6] Kimura H, Braun RD, Ong ET, Hsu R, Secomb TW, Papahadjopoulos D, Hong K, and Dewhirst MW (1996). Fluctuations in red cell flux in tumor microvessels can lead to transient hypoxia and reoxygenation in tumor parenchyma. *Cancer Res* **56**, 5522–5528.

[7] Weidner N, Semple JP, Welch WR, and Folkman J (1991). Tumor angiogenesis and metastasis—correlation in invasive breast carcinoma. *N Engl J Med* **324**, 1–8.

[8] Fox SB (1997). Tumour angiogenesis and prognosis. *Histopathology* **30**, 294–301.

[9] Gillies RJ, Schornack PA, Secomb TW, and Raghunand N (1999). Causes and effects of heterogeneous perfusion in tumors. *Neoplasia* **1**, 197–207.

[10] Semenza GL and Wang GL (1992). A nuclear factor induced by hypoxia *via de novo* protein synthesis binds to the human erythropoietin gene enhancer at a site required for transcriptional activation. *Mol Cell Biol* **12**, 5447–5454.

[11] Maxwell PH, Wiesener MS, Chang GW, Clifford SC, Vaux EC, Cockman ME, Wykoff CC, Pugh CW, Maher ER, and Ratcliffe PJ (1999). The tumour suppressor protein VHL targets hypoxia-inducible factors for oxygen-dependent proteolysis. *Nature* **399**, 271–275.

[12] Ivan M, Kondo K, Yang H, Kim W, Valiando J, Ohh M, Salic A, Asara JM, Lane WS, Kaelin Jr, WG (2001). HIFalpha targeted for VHL-mediated destruction by proline hydroxylation: implications for O_2 sensing. *Science* **292**, 464–468.

[13] Semenza GL (2001). HIF-1, O(2), and the 3 PHDs: how animal cells signal hypoxia to the nucleus. *Cell* **107**, 1–3.

[14] Semenza GL (1998). Hypoxia-inducible factor 1: master regulator of O_2 homeostasis. *Curr Opin Genet Dev* **8**, 588–594.

[15] Jaakkola P, Mole DR, Tian YM, Wilson MI, Gielbert J, Gaskell SJ, Kriegsheim A, Hebestreit HF, Mukherji M, Schofield CJ, et al. (2001). Targeting of HIF-alpha to the von Hippel-Lindau ubiquitination complex by O_2-regulated prolyl hydroxylation. *Science* **292**, 468–472.

[16] Semenza GL, Roth PH, Fang HM, and Wang GL (1994). Transcriptional regulation of genes encoding glycolytic enzymes by hypoxia-inducible factor 1. *J Biol Chem* **269**, 23757–23763.

[17] Ebert BL, Firth JD, and Ratcliffe PJ (1995). Hypoxia and mitochondrial inhibitors regulate expression of glucose transporter-1 *via* distinct *cis*-acting sequences. *J Biol Chem* **270**, 29083–29089.

[18] Maxwell PH, Dachs GU, Gleadle JM, Nicholls LG, Harris AL, Stratford IJ, Hankinson O, Pugh CW, and Ratcliffe PJ (1997). Hypoxia-inducible factor-1 modulates gene expression in solid tumors and influences both angiogenesis and tumor growth. *Proc Natl Acad Sci USA* **94**, 8104–8109.

[19] Wykoff CC, Beasley NJ, Watson PH, Turner KJ, Pastorek J, Sibtain A, Wilson GD, Turley H, Talks KL, Maxwell PH, et al. (2000). Hypoxia-inducible expression of tumor-associated carbonic anhydrases. *Cancer Res* **60**, 7075–7083.

[20] Levy AP, Levy NS, Wegner S, and Goldberg MA (1995). Transcriptional regulation of the rat vascular endothelial growth factor gene by hypoxia. *J Biol Chem* **270**, 13333–13340.

[21] Semenza GL (1994). Regulation of erythropoietin production. New insights into molecular mechanisms of oxygen homeostasis. *Hematol Oncol Clin North Am* **8**, 863–884.

[22] Zhong H, De Marzo AM, Laughner E, Lim M, Hilton DA, Zagzag D, Buechler P, Isaacs WB, Semenza GL, and Simons JW (1999). Over-expression of hypoxia-inducible factor 1alpha in common human cancers and their metastases. *Cancer Res* **59**, 5830–5835.

[23] Ross DT, Scherf U, Eisen MB, Perou CM, Rees C, Spellman P, Iyer V, Jeffrey SS, Van de Rijn M, Waltham M, et al. (2000). Systematic variation in gene expression patterns in human cancer cell lines. *Nat Genet* **24**, 227–235.

[24] Ellison G, Klinowska T, Westwood RF, Docter E, French T, and Fox JC (2002). Further evidence to support the melanocytic origin of MDA-MB-435. *Mol Pathol* **55**, 294–299.

[25] Sellappan S, Grijalva R, Zhou X, Yang W, Eli MB, Mills GB, and Yu D (2004). Lineage infidelity of MDA-MB-435 cells: expression of melanocyte proteins in a breast cancer cell line. *Cancer Res* **64**, 3479–3485.

[26] Schornack PA and Gillies RJ (2003). Contributions of cell metabolism and H^+ diffusion to the acidic pH of tumors. *Neoplasia* **5**, 135–145.

[27] Chen J, Zhao S, Nakada K, Kuge Y, Tamaki N, Okada F, Wang J, Shindo M, Higashino F, Takeda K, et al. (2003). Dominant-negative hypoxia-inducible factor-1 alpha reduces tumorigenicity of pancreatic cancer cells through the suppression of glucose metabolism. *Am J Pathol* **162**, 1283–1291.

[28] Welsh S, Williams R, Kirkpatrick L, Paine-Murrieta G, and Powis G (2004). Antitumor activity and pharmacodynamic properties of PX-478, an inhibitor of hypoxia-inducible factor-1alpha. *Mol Cancer Ther* **3**, 233–244.

[29] Forsythe JA, Jiang BH, Iyer NV, Agani F, Leung SW, Koos RD, and Semenza GL (1996). Activation of vascular endothelial growth factor gene transcription by hypoxia-inducible factor 1. *Mol Cell Biol* **16**, 4604–4613.

[30] Paweletz N and Knierim M (1989). Tumor-related angiogenesis. *Crit Rev Oncol Hematol* **9**, 197–242.

[31] Carmeliet P, Dor Y, Herbert JM, Fukumura D, Brusselmans K, Dewerchin M, Neeman M, Bono F, Abramovitch R, Maxwell P, et al. (1998). Role of HIF-1alpha in hypoxia-mediated apoptosis, cell proliferation and tumour angiogenesis. *Nature* **394**, 485–490.

[32] Sourvinos G, Miyakis S, Liloglou TL, Field JK, and Spandidos DA (2001). Von Hippel-Lindau tumour suppressor gene is not involved in sporadic human breast cancer. *Tumour Biol* **22**, 131–136.

[33] Chan DA, Sutphin PD, Denko NC, and Giaccia AJ (2002). Role of prolyl hydroxylation in oncogenically stabilized hypoxia-inducible factor-1alpha. *J Biol Chem* **277**, 40112–40117.

[34] Karni R, Dor Y, Keshet E, Meyuhas O, and Levitzki A (2002). Activated pp60c-Src leads to elevated hypoxia-inducible factor (HIF)-1alpha expression under normoxia. *J Biol Chem* **277**, 42919–42925.

[35] Minet E, Mottet D, Michel G, Roland I, Raes M, Remacle J, and Michiels C (1999). Hypoxia-induced activation of HIF-1: role of HIF-1alpha–Hsp90 interaction. *FEBS Lett* **460**, 251–256.

[36] Isaacs JS, Jung YJ, Mimnaugh EG, Martinez A, Cuttitta F, and Neckers LM (2002). Hsp90 regulates a von Hippel Lindau–independent hypoxia-inducible factor-1 alpha-degradative pathway. *J Biol Chem* **277**, 29936–29944.

[37] Lu H, Forbes RA, and Verma A (2002). Hypoxia-inducible factor 1 activation by aerobic glycolysis implicates the Warburg effect in carcinogenesis. *J Biol Chem* **277**, 23111–23115.

[38] Bos R, van Der Hoeven JJ, van Der Wall E, van Der Groep P, van Diest PJ, Comans EF, Joshi U, Semenza GL, Hoekstra OS, Lammertsma AA, et al. (2002). Biologic correlates of (18)fluorodeoxyglucose uptake in human breast cancer measured by positron emission tomography. *J Clin Oncol* **20**, 379–387.

[39] Gatenby RA and Gawlinski ET (2003). The glycolytic phenotype in carcinogenesis and tumor invasion: insights through mathematical models. *Cancer Res* **63**, 3847–3854.

[40] Berggren M, Gallegos A, Gasdaska JR, Gasdaska PY, Warneke J, and Powis G (1996). Thioredoxin and thioredoxin reductase gene expression in human tumors and cell lines, and the effects of serum stimulation and hypoxia. *Anticancer Res* **16**, 3459–3466.

[41] Pfaffl MW (2001). A new mathematical model for relative quantification in real-time RT-PCR. *Nucleic Acids Res* **29**, e45.